Optical and photoemission studies of TmTe

R. Suryanarayanan,* G. Güntherodt,† J. L. Freeouf,‡ and F. Holtzberg

IBM T. J. Watson Research Center, Yorktown Heights, New York 10598

(Received 9 June 1975)

We report here on the optical absorption of TmTe films ($5 < T < 300$ K; $0.2 < h\nu < 4.5$ eV) and the reflectance ($0.2 < h\nu < 20$ eV) and ultraviolet photoemission spectra (UPS; $15 \le h\nu \le 90$ eV) of vacuum- and air-cleaved TmTe single crystals. Much of the structure seen in absorption and reflectance spectra can be attributed to transitions from Tm^{2+}, e.g., the first absorption band centered at 0.7 eV is identified as due to a transition from Tm^{2+} $4f^{13} \rightarrow 4f^{12}(^3H_6)5d(t_{2g})$. No optical structure was seen which would permit us to identify Tm^{3+} in TmTe. The UPS data show a small amount of Tm^{3+} which was, however, strongly influenced by surface conditions in spite of *in situ* study in a vacuum of 10^{-10} Torr. We conclude that Tm is essentially divalent in TmTe.

I. INTRODUCTION

The monochalcogenides of rare-earth elements, crystallizing in the NaCl structure, exhibit interesting electrical, optical, and magnetic properties. Among these, the monochalcogenides of Eu (f^7, half filled), Yb (f^{14}, fully filled), Sm (f^6, nearly half filled), and Tm (f^{13}, nearly fully filled) attract particular attention because of their divalent character in certain compounds. However, Tm has been reported to be trivalent in TmS, and further, is reported[1] to have a fluctuating valency between 2 and 3 in TmSe and TmTe at room temperature and at atmospheric pressure, as deduced from the x-ray photoemission spectra (XPS). On the other hand, TmTe is found to undergo an isostructural semiconductor-metal (S-M) transition[2] under pressure around 40 kbar at room temperature, which is explained as due to a transformation of Tm^{2+} to Tm^{3+}.

Since TmTe exists over a wide range of stoichiometries, and many of its properties are strongly stoichiometry dependant,[3] we first discuss the preparation and characterization of our samples of TmTe (Sec. II). We next present the results of our optical and photoemission studies of these samples (Sec. III). In Sec. IV we discuss optical-absorption processes involving localized f levels, and construct an energy-level diagram consistent with our results. Finally, we argue that available evidence strongly implies an essentially pure divalent ground state for Tm in TmTe.

II. SAMPLE PREPARATION AND CHARACTERIZATION

A. Single crystals

Stoichiometric amounts of Tm ingots (99.99%) and Te (99.9995%) were placed at the two ends of an evacuated quartz tube. This was enclosed in another quartz tube and the interspace continuously flushed with He gas. The reaction was carried out by transporting Te vapor to the Tm metal over several days during which the temperature was gradually raised to 800 °C. This product was powdered, pressed into pellets, and heated in a vacuum-sealed tungsten crucible in a rf vacuum furnace to 1650 °C for 3–4 h. The contents of the crucible were analyzed chemically. A correction was made to account for stoichiometric deficiency, and the product was again placed in a tungsten crucible and heated to 2350 °C for 4 h. The temperature was reduced to 1850 °C (in 5–7 h), where it was maintained for about 8 h, and then brought to room temperature in 1 or 2 h. The crystals thus obtained looked black with some patches of dull grey color. However, the cleaved-crystal surface looked uniformly black. A cleaved crystal washed in water slowly developed greyish and silvery patches.

The lattice constant a calculated from the powder photograph (Guinier camera) as well as from x-ray reflections from a single crystal (in Eulerian geometry) was 6.340 ± 0.001 Å, and the electron microprobe analysis gave a composition stoichiometric within the 2% accuracy of the analyses. The lattice constant obtained agrees well with the earlier value reported[4] for TmTe. From the measurements by Iandelli *et al.*[4] of the lattice constants of powder samples for $TmTe_x$ ($0.9 < x < 1.05$), one could estimate $a = 6.340$ Å for a stoichiometric composition, which suggests that our single-crystal samples were very close to being stoichiometric.

B. Films

TmTe pellets (sintered at 1650 °C) were evaporated by electron beam heating in a vacuum of 5×10^{-6} Torr onto heated (~ 350 °C) substrates of quartz and CaF_2. Table I summarizes some of the properties of the films. Films obtained on successive evaporation runs had notably different lattice constants; presumably this was due to a change in composition of the films. The films had a tendency to oxidize if left in moist air, as evidenced by an increase in oxygen counts in an elec-

TABLE I. Some properties of TmTe films crystallizing in NaCl structure. All films are on quartz, except Samples No. S-12 and No. G-12 which are on CaF_2.

| | | | Color | | |
Sample	Thickness (Å)	Lattice constant (Å)	Transmission	Reflection	Composition
F-14	5000	6.335 ± 0.004	greenish yellow	black	$Tm_{49\pm1}Tm_{50\pm1}$
S-12	4500	6.30 ± 0.005	orange brown	dark gray	
G-12	...	6.31 ± 0.005	greenish brown	black	
R-18	5600	6.32 ± 0.008	red	blue	
M-17	...	Two NaCl phases 6.29, 6.10	deep orange	blue	

tron microprobe analysis. These oxidized films then look bluish in reflection. The lattice constant of sample No. F-14 (6.335 ± 0.004 Å, NaCl structure) is very close to that of a stoichiometric single crystal. In one of the runs, we obtained a film having two NaCl phases with $a = 6.29$ and 6.10 Å, as has also been observed in the case of powder samples.[4]

III. RESULTS

A. Optical absorption of films

The optical absorption of TmTe films was measured as a function of temperature $5 < T < 300$ K, and in the photon energy range $0.20 < h\nu < 4.5$ eV, using Cary 14 and Perkin-Elmer 301 spectrophotometers. The first absorption band is located around 0.7 eV in all the samples (except M-17 which was a two-phase sample). For film No. F-14, which is essentially a stoichiometric sample (see Sec. IIB), the absorption coefficient at 0.7 eV is $\simeq 2 \times 10^4$ cm^{-1}, neglecting reflection
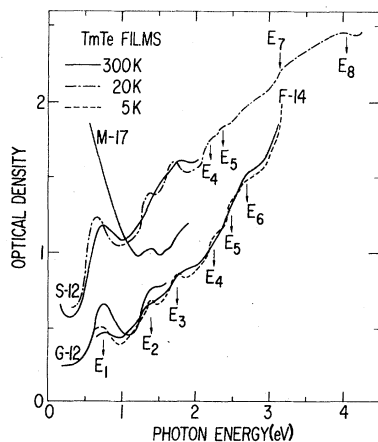
loss. The absorption coefficient is found to increase upon cooling, starting around 200 K. A sizeable red shift is found for the E_1 maximum (see Table II). There is no change in the spectrum in Fig. 1 in the range $5 < T < 20$ K. For $T < 20$ K the absorption bands E_2 and E_3 are clearly resolved. Further maxima are seen superimposed on a continuously rising background absorption up to 4.5 eV. Whereas the absorption decreases towards the infrared for film No. G-12, it shows an increase for No. S-12 starting from 0.3 eV, owing to free carrier absorption. The free carriers are probably due to the deviations from stoichiometry. This increase in absorption with decreasing photon energy starts much earlier, around 1.75 eV, in the two-phase film No. M-17.

B. Reflectance

The room-temperature reflectance of cleaved single crystals of TmTe has been measured for photon energies from 0.05 to 20 eV. In the spectral region from 2 to 20 eV the reflectance[5] measurements were carried out at the 240-MeV electron storage ring of the University of Wisconsin Physical Sciences Laboratory. One sample was cleaved *in situ* in a vacuum of better than 2×10^{-8}

FIG. 1. Optical density of TmTe films.

TABLE II. Some of the positions of absorption maxima in eV (± 0.03) of TmTe films and single crystal.

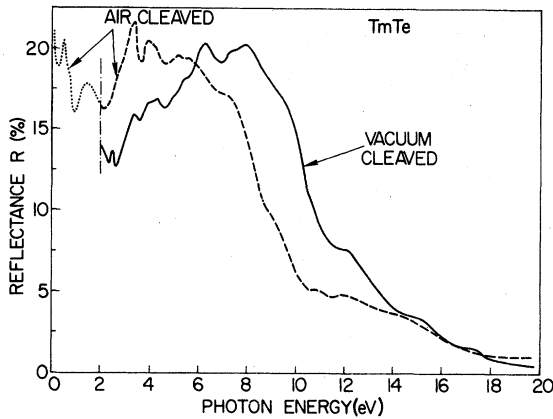| Sample		E_1	E_2	E_3	E_4	E_5
F-14	300 K	0.75	1.37	1.80		
	5 K	0.70	1.40	1.75	2.25	2.45
S-12	300 K	0.73		1.79		
	20 K	0.66	1.40	1.67	2.19	2.38
TmTe single crystal						
	300 K	0.70	1.30	1.75	2.22	2.48

FIG. 2. Reflectance of air-cleaved (dotted line and dashed line) and vacuum-cleaved (solid line) TmTe single crystals at 293 K.

Torr. For photon energies from 0.05 to 2 eV, air-cleaved samples were measured in an inert-gas atmosphere using Perkin-Elmer 301 and Cary 14 spectrophotometers. In order to study the effect of surface oxidation on the optical properties, we have also measured an air-cleaved sample (~1 h between cleave and measurement in vacuum) for photon energies from 2 to 20 eV.

Figure 2 shows the reflectance spectrum of vacuum-cleaved TmTe from 2 to 20 eV (solid line). The spectrum shows detailed and pronounced structure up to 8 eV, followed by a strong decrease with increasing photon energy to almost zero at 20 eV. The same measurement on an air-cleaved
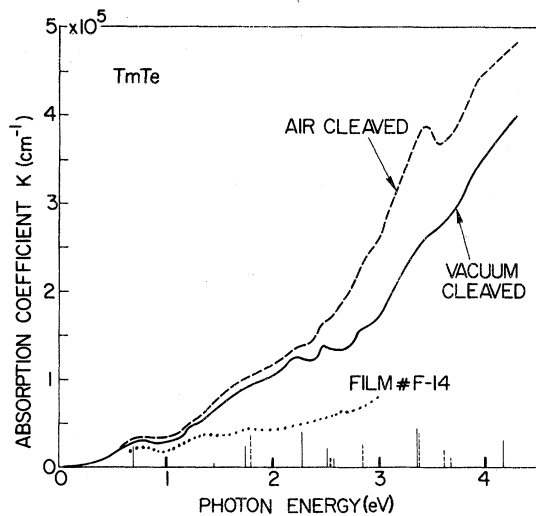

FIG. 3. Absorption coefficient of air cleaved (dashed line) and vacuum cleaved (solid line) TmTe single crystals at 293 K. Calculated relative strenghts of optical transitions $4f^{13} \rightarrow 4f^{12}5dt_{2g}$ (solid line) and $4f^{13} \rightarrow 4f^{12}5d_{eg}$ (dashed line) are shown on the abscissa.
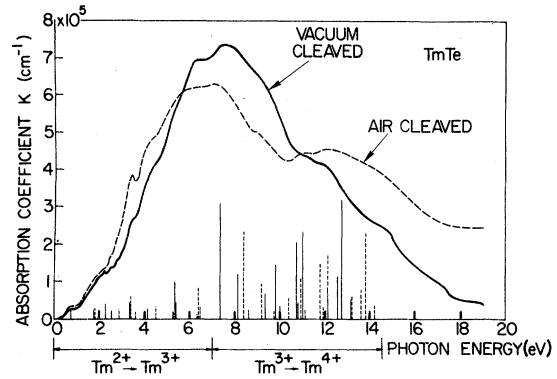

FIG. 4. Absorption coefficient of air-cleaved (dashed line) and vacuum-cleaved TmTe single crystals at 293 K. Calculated relative strengths of optical transitions $4f^{13}(Tm^{2+}) \rightarrow 4f^{12}5dt_{2g}$ (solid line) and $4f^{13} \rightarrow 4f^{12}5d_{eg}$ (dashed line) as well as $4f^{12}(Tm^{3+}) \rightarrow 4f^{11}5dt_{2g}$ (solid line) and $4f^{12} \rightarrow 4f^{11}5d_{eg}$ (dashed line) are shown on the abscissa (calculated intensities should only be compared to others from the same ground state, i.e., the scale for Tm^{2+} lines is not related to the scale for Tm^{3+} lines.

sample (dashed line) shows an increase in reflectivity between 2 and 5 eV, followed by a much stronger decrease above 5 eV compared to the reflectivity of vacuum-cleaved TmTe. The exposure of the crystal surface to air makes the reflectivity peaks of vacuum-cleaved TmTe at 2.5, 6, and 8 eV disappear, whereas it enhances the peak around 3.3 eV. Thus it is evident that the reflectivity of TmTe is strongly affected by the exposure of the crystal surface to air. For photon energies from 0.05 to 2 eV the reflectivity of an air-cleaved sample (dotted line) shows two distinct maxima at 0.5 and 1.4 eV. The increasing reflectivity below 0.25 eV indicates the free-carrier absorption, which depends on the stoichiometry of the samples.

The reflectivity shown in Fig. 2 has been analyzed in terms of the optical constants by means of the Kramers-Kronig relation. Above 20 eV the reflectivity has been extrapolated by $R \sim 1/\omega^4$. In order to extrapolate the reflectance of vacuum-cleaved TmTe below 2 eV, we have matched it at 2 eV with that of an air-cleaved sample for 0.05-2 eV. The calculated absorption coefficient is shown in Figs. 3 and 4 for vacuum-cleaved TmTe (solid line) and air-cleaved TmTe (dashed line). In both cases the absorption coefficient of vacuum-cleaved TmTe increases with increasing photon energy up to a maximum around 8 eV. At higher energies, a monotonic decrease to almost zero at 20 eV is observed. The broad absorption maximum around 8 eV in vacuum-cleaved TmTe is lower in amplitude and slightly shifted towards lower photon energies compared with air-cleaved
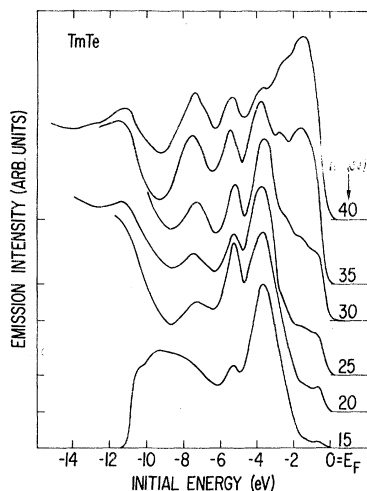
FIG. 5. Photoelectron energy distributions for a cleaved single crystal of TmTe. For $15 \leq h\nu \leq 40$ eV. Energies are referred to the Fermi level, $E_F = 0$.

TmTe. In the latter case the most striking feature is the appearance of an additional broad maximum around 12 eV. The structure in the absorption spectrum of vacuum-cleaved TmTe can still be seen for the air-cleaved sample, although it becomes more smeared out.

C. Photoemission

Photoelectron energy distributions (PED's) were measured in the range $10 \lesssim h\nu \lesssim 90$ eV using synchrotron radiation (at the University of Wisconsin PSL storage ring) and a previously described photoemission spectrometer system.[6] Single crystals of TmTe of area ~4 mm² were cleaved [(100) face] and measured *in situ* at pressures of $\lesssim 6 \times 10^{-10}$ Torr.

Figure 5 shows PED's for TmTe at various values of $h\nu$. Note that the onset of emission is ~0.25 eV below the Fermi level E_F, i. e., there is no emission at E_F; this implies that TmTe is a semiconductor. As Figure 5 shows, relative emission intensity near E_F increases dramatically as $h\nu$ is increased from 15 to 40 eV. This leads us to assign these features to emission from the localized f levels of the Tm ion, since emission from f levels is weak relative to that of p-like bonding valence-band (VB) levels at low values of $h\nu$ and increases in relative strength with increasing $h\nu$.[7]

We can therefore use the PED's for low photon energies to study the density of bonding valence-band states. We would place the VB edge E_v ~1.7 eV (± 0.3 eV) below E_F with peaks at 3.6, 5.2, and 7.3 eV, and with edges at 4.3, 5.7, and 7.9 eV (all ± 0.2 eV) below E_F, and believe the upper three VB's to be ~6 eV wide. This VB den-

sity of states is characteristic of many tellurides, i. e., similar width and relative intensities to, e. g.,[6] CdTe (zinc-blende structure) at the same photon energy. Conversely, the f-level emission is best studied at relatively high photon energies $h\nu \gtrsim 40$ eV; Fig. 6 shows such data at $h\nu = 50$ eV. Virtually all of the structures shown can be assigned to emission from the localized f electrons, as is indicated at the bottom of the figure. The details of these assignments will be discussed later; at this point we wish only to point out that we clearly see and identify emission from both divalent and trivalent Tm, and the ratio $r = I(\text{Tm}^{3+})/I(\text{Tm}^{2+})$ is strongly time dependent despite ultrahigh-vacuum (UHV) *in situ* preparation and study. The lowest value we have observed for this ratio is $r = 0.06$ (4 min after cleave). The experimental scatter is such that ratios between $r = 0.13$ and 0.19 (at ~8–9 min after the cleave depending on cleave) have been observed. This ratio appears insensitive to the photon energy used ($50 \leq h\nu \leq 85$ eV).

IV. DISCUSSION

A. Optical-absorption processes involving f levels

Optical-absorption processes (including photoemission) involve (by Fermi's golden rule) a joint density of states (JDS) multiplied by the dipole matrix element squared. The dipole operator is a one-electron operator; the use of band theories of solids is predicated upon this matrix element and the JDS being independent of the electrons that are not directly involved in this excitation. Most VB states in solids are sufficiently delocal-
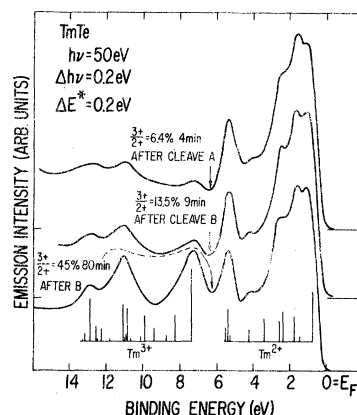

FIG. 6. Photoelectron energy distribution for cleaves A and B of the single crystals of TmTe at $h\nu = 50$ eV. Electron energies are referred to the Fermi level E_F. Emission expected from f levels of Tm^{2+} and Tm^{3+} is indicated in the lower part of the figure (see text). Time dependence of emission from $\text{Tm}^{3+} f$ levels suggests that sample contamination occurred quickly even at our pressure of $\lesssim 6 \times 10^{-10}$ Torr.

ized that this is a reasonably good approximation, an exception being transitions near the fundamental gap in which electron-hole (excitonic) interactions can become important. In the case of highly correlated atomiclike levels (such as $4f$ levels) this approximation is very poor; the hole may be left behind in different states, each having a different energy and a different probability of occurrence.

Atomic spectroscopists have dealt with these systems for many years; they have determined the energy of each hole state,[8] and developed a formalism[9] which we have exploited[10] to compute the relative intensities of optical absorption of $4f$ levels.

The relative intensities may be calculated by using coefficients of fractional parentage.[11,12] This permits us to write an n-electron wave function as the sum of products of $(n-1)$- and 1-electron wave functions, i.e.,

$$|I\rangle \equiv |4f^n SLJM_J\rangle$$

$$= \sum \langle 4f^{n-1}S'L'J'M'_J; \tfrac{1}{2}3jm_j|4f^n SLJM_J\rangle$$

$$\times |4f^{n-1}S'L'J'M'_J\rangle \, |\tfrac{1}{2}3jm_j\rangle \,,$$

where the coefficients

$$\langle 4f^{n-1}S'L'J'M'_J; \tfrac{1}{2}3jm_j|4f^n SLJM_J\rangle$$

are easily obtained from tabulated coefficients of fractional parentage (and Clebsch-Gordan coefficients to transform them to the $|SLJM_J\rangle$ representation). Any final state $|F\rangle$ for a one-electron transition from the f^n ground state can similarly be expanded

$$|F\rangle = \sum \langle 4f^{n-1}S''L''J''M''_J; \alpha|F\rangle$$

$$\times |4f^{n-1}S''L''J''M''_J\rangle|\alpha\rangle \,,$$

where $|\alpha\rangle$ is the excited electron wave function (to be discussed later).

The optical matrix element X is then easily obtained[13]

$$X = n \sum \langle 4f^{n-1}S'L'J'M'_J; \alpha|F\rangle$$

$$\times \langle 4f^{n-1}S'L'J'M'_J; \tfrac{1}{2}3jm_j|I\rangle \langle \alpha|\vec{A}\cdot\vec{P}|\tfrac{1}{2}3jm_j\rangle.$$

Thus far the derivation has been rather general and rigorous. We now make some approximations as to the nature of $|\alpha\rangle$, namely, we expand the part of the final excited electron state to which the initial state is coupled by $\vec{A}\cdot\vec{P}$ (plane-wave-like for photoemission, t_{2g} for optical absorption) in terms of atomic d orbitals. In this case we can write the coefficients $\langle 4f^{n-1}S'L'J'M'_J; \alpha|F\rangle$ as Clebsch-Gordan coefficients. Within these assumptions we have calculated all matrix elements in terms of one reduced matrix element.[14]

We obtain a line shape for exciting one electron

from the n-(f-electron) ground state to either a t_{2g} state (optical absorption) or a plane-wave-like state (photoemission) by combining our calculated relative intensities with the energy separations determined by atomic spectroscopists. Figure 6 of Sec. III shows these results for photoemission from both Tm^{2+} ($n=13$) and Tm^{3+}($n=12$).

B. Interpretation of absorption data and ($\hbar\omega < 4.5$ eV) energy-level scheme for divalent TmTe

In the absence of any available band-structure calculation, let us assume the model proposed for Eu chalcogenides[15] to be valid for divalent TmTe. In this model, the $4f$ levels of Tm would be between the valence and conduction bands formed, respectively, by the p orbitals of the chalcogen and $5d$-$6s$ orbitals of Tm. The optical absorption will originate from $4f^{13}(Tm^{2+}) \to 4f^{12}5d$ transitions in addition to the usual valence-conduction-band transitions. The ground state of Tm^{2+} is $^2F_{7/2}$ with a spin-orbit-split $^2F_{5/2}$ lying at ~1.24 eV above it. In O_h symmetry, $^2F_{7/2}$ is split by the crystal field into Γ_6, Γ_7, and Γ_8 states of which the Γ_7 is the lowest state, and we consider transitions from $4f^{13}(^2F_{7/2}, \Gamma_7) \to 4f^{12}5d$.

The excited $4f^{12}5d$ state is subject to the following interactions: $H_{cf}(d)$, the crystal field of Te^{--} ions separates the d levels by $10Dq$ into a t_{2g} (Γ_5) and e_g (Γ_3), the former lying lower in energy. The Coulomb interaction between f electrons $H_{el}(f)$ results in terms ^3H, ^3F, ^1G, etc. The spin-orbit interaction $H_{so}(f)$ further splits them into $^3H_6$, $^3H_4$, $^3H_5$, $^3F_4$, $^3F_3$, $^3F_2$, $^1G_4$, $^1D_2$ situated, respectively, at 0, 0.7, 1.05, 1.6, 1.74, 1.87, 2.63, and 3.40 eV.[8] We neglect the interaction $H_{so}(d)$ ($\simeq 0.2$ eV for a free ion) and $H_{el}(fd)$, the Coulomb interaction between f and d electrons. Let us note that this latter interaction has been taken into account to explain the Tm^{2+} spectra in $SrCl_2$,[16] whereas it was neglected in the explanation of the spectra of Yb^{2+} in $SrCl_2$,[17] $YbTe$,[18] EuF_2,[19] and $SmTe$.[20]

We can estimate a $10Dq$ value of 1 eV for TmTe similar to that of YbTe,[18] based on the fact that the lattice constants and the ionic radii of Tm^{2+} and Yb^{2+} are similar. We see then $H_{el}(f)$, $H_{so}(f)$, and $10Dq$ are of the same order of magnitude and this would complicate a detailed interpretation of the spectrum. However, we start by noting that $E_2 - E_1 \simeq 0.7$ eV and is close to the separation between $^3H_6$ and $^3H_4$, and hence it is tempting to assign the band at E_1 due to transitions $4f^{13}(^2F_{7/2}) \to 4f^{12}(^3H_6)5d(t_{2g})$ and E_2 to $4f^{13} \to 4f^{12}(^3H_4)5d(t_{2g})$ (Fig. 7). The excited states have the right symmetry for an allowed electric dipole transition, as can be checked by group theory [e.g., t_{2g} (Γ_5) $\otimes H_{so}(d)$ (Γ_6) $\otimes {}^3H_6$ ($^2\Gamma_3$) $= \Gamma_7 + \cdots$]. Note further that $E_5 - E_3 \simeq 0.7$ eV and that $E_5 - E_2 \simeq E_3 - E_1$
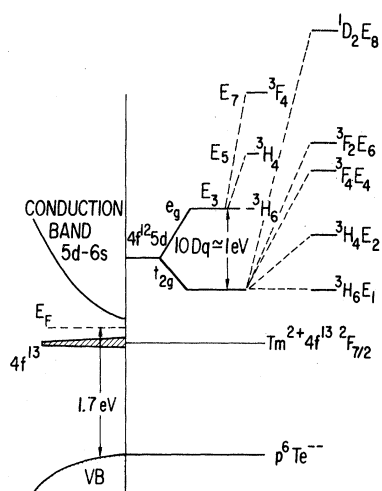
FIG. 7. Schematic energy-level diagram for $Tm^{2+}Te$.

$\simeq 1.05$ eV, which is of the order of $10Dq$ expected for TmTe. Hence one could assign E_3 to $4f^{13}$ $\rightarrow 4f^{12}$ ($^3H_6$)e_g and E_5 to $4f^{13} \rightarrow f^{12}$ ($^3H_4$)e_g. By similar arguments, one can assign tentatively the other maxima labeled up to E_8 (see Fig. 7). The region beyond 2.5 eV contains valence-conduction–band transitions and transitions of the type $4f^{13}$ $\rightarrow 4f^{12}$ ($^3H_6$)$6s$ which has a Γ_8 symmetry.[21]

C. Comparison of optical absorption with calculated 4f-level intensities

In Figs. 3 and 4 we compare the absorption coefficient of air- and vacuum-cleaved TmTe with the above calculated intensities of the excited $4f$ configurations (Sec. IV A) of di- and trivalent Tm. The first multiplet level, belonging to divalent Tm and representing the transition $4f^{13} \rightarrow 4f^{12}$ ($^3H_6$)$5dt_{2g}$, has been fixed at the first absorption band around 0.7 eV, by which the whole set of multiplet levels of divalent Tm up to 5.3 eV (solid lines) is fixed in energy. In order to take into account the crystal-field splitting of the $5d$ states, the multiplet level set has been shifted rigidly up to higher photon energies (dashed lines), and each level has been multiplied by $\frac{2}{3}$ to account for the different level degeneracy of $5dt_{2g}$ and $5de_g$ states. Best agreement between structure in the absorption spectrum and calculated $4f$ levels, concerning their position in energy, has been achieved for 10 $Dq \simeq 1.1$ eV. This is in good agreement with our above estimated value. A comparison of the magnitude of the absorption with the calculated intensity of the $4f$ levels is impossible because of the superimposed background absorption due to valence-to-conduction–band transitions. The latter has an onset at about 1.7 eV as deduced from our photoemission data. The width of the p

derived valence band (6 eV) accounts mainly for the broad maximum in the absorption around 7 eV as seen in Fig. 4. The set of multiplet levels for trivalent Tm has been fixed with its lowest level at 7.3 eV according to the Coulomb correlation energy as determined from our photoemission data. The same crystal-field splitting of $10Dq = 1.1$ eV as above has been used. Because of the large penetration depth of the light of 100–1000 Å ($K = 10^6 - 10^5$ cm^{-1}) we do not consider it very likely that the structure in the absorption of vacuum-cleaved TmTe above 7 eV is related to trivalent Tm, assuming an average time of measurement of 1 h after cleaving. Furthermore we see that the agreement between structure in the absorption and the position in energy of calculated $4f$ levels in the region from 7 to 14 eV is not very good, contrary to the assignment for divalent Tm. The exposure of the sample surface to air modifies mainly the background absorption, with the structure of the absorption of vacuum-cleaved TmTe still retained but slightly smeared out. Below 7 eV the background of the absorption spectrum of air-cleaved TmTe seems to be shifted towards lower photon energies with respect to that of vacuum-cleaved TmTe. This can be due to a smaller gap between the valence and conduction bands or a band tailing because of disorder at the surface of the sample. While the absorption of air-cleaved TmTe is reduced for $5 < h\nu < 11$ eV compared to vacuum-cleaved TmTe, it is enhanced for photon energies above 11 eV owing to the appearance of a broad maximum around 12 eV. We
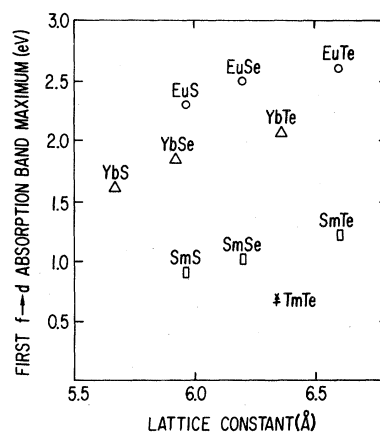

FIG. 8. Relation between the lattice constants of divalent rare-earth chalcogenides and the first $f \rightarrow d$ absorption-band maxima. References: EuX (Ref. 16); YbTe, YbSe (Ref. 18); YbS, J. B. Torrance and F. Holtzberg (unpublished); SmTe, SmSe (Ref. 20); SmS, F. Holtzberg and J. B. Torrance, AIP Conf. Proc. 5, 860 (1972); TmTe predicted value +, observed value × (this work).

notice that for air-cleaved TmTe there is no new detailed structure appearing in the absorption compared with vacuum-cleaved TmTe. Hence a comparison with the calculated $4f$ levels of trivalent Tm does not result in a conclusive assignment.

D. Relation between TmTe and other divalent rare-earth chalcogenides

In order to compare the divalent character of TmTe with the other known divalent rare-earth chalcogenides, we have plotted the lattice constants of EuX, SmX, YbX (X = S, Se, Te) with the first $f \rightarrow d$ absorption-band maxima E_1 obtained from the optical absorption of thin films of the respective compounds (Fig. 8). We note that E_1 of the Sm chalcogenides lies at about 1.5 eV vertically below the respective E_1 of the Eu chalcogenides. If we assume a similar relationship between YbTe and TmTe (the analogs of EuTe and SmTe) we get a value of 0.65 eV for TmTe as the first $f \rightarrow d$ absorption-band maximum, which is close to the observed value of 0.7 eV. A similar argument cannot be put forward by comparing YbSe and TmSe or YbS and TmS since their respective lattice constants are considerably different (cf., $a_{YbSe} = 5.93$, $a_{TmSe} = 5.71$; $a_{YbS} = 5.68$, $a_{TmS} = 5.41$) and these materials (TmSe and TmS) are not divalent chalcogenides.

E. Semiconductor-metal (S-M) transition in TmTe

We estimate an $f \rightarrow d$ band gap of about 0.35 eV from our absorption data. If this gap moves at a rate of -11 meV/kbar (similar to that of[22] YbTe), then a S-M transition would occur at around 40 kbar as has been reported.[2]

F. Arguments to support the presence of only divalent Tm in TmTe

1. Lattice constant

The lattice constant is a good measure of the valence state of a rare-earth ion in a compound. The lattice constant of TmTe, $a = 6.34$ Å, is very close to that expected for Tm^{2+} Te if we compare it with the lattice constant of Yb^{2+} Te ($a = 6.36$ Å).

2. Magnetic susceptibility

The valence state and the magnetic properties of the Tm monochalcogenides have been discussed recently.[1,3,23,24] One of the puzzling results concerns the fact that the magnetic long-range order below the ordering temperature (TmTe, T_N = 0.21 K) could not be detected by neutron diffraction, but was clearly observed by low-temperature specific heat, magnetization, susceptibility, thermal expansion, and magnetostriction.[3,23,24] In the case of TmTe, the question is whether the

ground state is purely $4f^{13}$ or a mixture of $4f^{13}$ and $4f^{12}$ $(5d6s)$.[1] In the latter case the measured susceptibility can be described[25] by $\chi_m = \langle \mu^2 \rangle / (3kT + \Delta)$, where $\langle \mu^2 \rangle$ is a weighted average of the squared effective moments in both the valence states and $\Delta = \pi |V|^2 N(\epsilon_F)$, with V as the matrix element mixing the two states $4f^{13}$ and $4f^{12}$ $(5d6s)$.[1] Bucher et al.[3] fitted the measured susceptibility with $\Delta = 0$ implying the divalent Tm in TmTe. They obtained a value of $\mu_B = 4.96$, which is somewhat greater than 4.5, the value expected for Tm^{2+}. The deviation of μ_B from the expected value could be due to deviations from stoichiometry. Iandelli et al.[4] have measured the susceptibility of $TmTe_x$ for $0.9 < x < 1.25$ and found the effective magnetic moment to depend on the stoichiometry; the lowest value they obtained was $\mu_B = 4.63$ for $x = 0.98$. In general, it should be pointed out that deviations from stoichiometry certainly play a very important role. A very similar problem has been encountered and resolved in the case of Gd monochalcogenides.[26,27]

3. Elastic constant measurements

The elastic constants of TmTe have been measured for $4 < T < 300$ K by Lüthi et al.[28] The authors were able to explain fairly well their results at least for $T < 100$ K by assuming a Tm^{2+} configuration.

4. Photoemission and reflectance

The most striking evidence for the absence of any mixed valence state in TmTe comes, of course, from our uv photoemission experiments. Our results clearly indicate, as discussed above, that the amount of detectable Tm^{3+} in these experiments depends strongly on the surface condition. In fact, our observations of UPS show clearly that the ratio ratio[29] of Tm^{3+}/Tm^{2+} increases after cleavage as a function of time from a value of $\leq 6\%$ and thus points out that the earlier conclusion[1] based on x-ray photoemission measurements regarding a "mixed valence" state for Tm in TmTe were the result of neglecting the effect of surface oxidation. Also, the absorption spectrum of vacuum-cleaved TmTe, as derived from the reflectance, shows clear evidence for transitions from Tm^{2+} in the energy region 0–7 eV, but no conclusive indication of transitions from Tm^{3+} in the energy region 7–14 eV.

V. CONCLUSIONS

We have measured the optical absorption of TmTe films, reflectance, and uv photoemission of TmTe single crystals. The first absorption band centered around 0.7 eV in TmTe is attributed to transitions arising from $4f^{13} (Tm^{2+}) \rightarrow 4f^{12} (^3H_6)$

$\times 5dt_{2g}$. An estimated $f \to d$ gap of around 0.35 eV explains the semiconductor-metal transition observed under pressure (40 kbar).[2] Further transitions arising from $4f^{13} \to 4f^{12}(^{3}H_J, \, ^{3}F_J)$ $\times 5d(t_{2g}, e_g)$ can be identified yielding $10Dq \simeq 1$ eV. Whereas most of the structure seen in the absorption and reflectance spectra can be attributed to transitions from Tm^{2+} – or Te-derived valence bands, no structure is seen up to 20 eV which would permit us to identify Tm^{3+}. And finally our observations of uv photoemission from vacuum-cleaved TmTe show definitely that the amount of Tm^{3+} detectable is strongly influenced by the sur-face conditions, in spite of the *in situ* study in a vacuum of $<10^{-9}$ Torr, thus leading us to postulate a pure divalent ground state for Tm in TmTe.

*Present address: Laboratoire de Physique des Solids, C. N. R. S. , 92190- Bellevue, France.

†Present address: Max-Planck Institute für Festkörper-forschung, Heilbronner strasse 69, 7000 Stuttgart 1, W. Germany.

‡Supported in part by the U. S. Air Force Office of Scientific Research under Contract No. F44620-70-C-0089, and by the NSF under Contract No. DMR-74-15089.

[1] M. Campagna, E. Bucher, G. K. Wertheim, D. N. E. Buchanan, and L. D. Longinotti, Phys. Rev. Lett. **32**, 885 (1974).

[2] A. Jayaraman, E. Bucher, and D. B. McWhan, in *Proceedings of 8th Rare Earth Research Conference* (U. S. GPO, Washington, D.C. 1970), Vol. 1, p. 333.

[3] E. Bucher, K. Andres, F. J. diSalvo, J. P. Maita, A. C. Gossard, A. S. Cooper, and G. W. Hull, Jr., Phys. Rev. B **11**, 500 (1975).

[4] A. Iandelli and A. Palenzona, Colloq. Int. Cent. Natl. Rech. Sci. **1**, 397 (1967).

[5] The alignment procedures required for high absolute accuracy were not followed. The system is described by G. W. Rubloff, H. Fritzsche, U. Gerhardt, and J. L. Freeouf, Rev. Sci. Instrum. **42**, 1507 (1971).

[6] D. E. Eastman, W. D. Grobman, J. L. Freeouf, and M. Erbudak, Phys. Rev. B **9**, 3473 (1974).

[7] D. E. Eastman and Moshe Kuznietz, Phys. Rev. Lett. **26**, 846 (1971).

[8] G. H. Dieke and H. M. Crosswhite, Appl. Opt. **2**, 675 (1963).

[9] G. Raccah, Phys. Rev. **76**, 1352 (1949).

[10] J. L. Freeouf, D. E. Eastman, W. D. Grobman, F. Holtzberg, and J. B. Torrance, Phys. Rev. Lett. **33**, 161 (1974).

[11] P. A. Cox, Y. Baer, and C. K. Jorgensen, Chem. Phys. Lett. **22**, 433 (1973).

[12] These coefficients are tabulated in C. W. Nielson and G. F. Koster, *Spectroscopic Coefficients for the p^n, d^n, and f^n Configurations* (MIT Press, Cambridge, 1963).

[13] See, e.g., B. R. Judd, *Operator Techniques in Atomic Spectroscopy* (McGraw-Hill, New York 1963), p. 167.

[14] This involves a variant of the Wigner-Eckhart Theorem; see, e.g., A. Messiah, *Quantum Mechanics* (Wiley, New York, 1966), Vol. II, p. 1077.

[15] S. Methfessel, Z. Angew. Phys. **18**, 414 (1965); S. Methfessel, F. Holtzberg, and T. R. McGuire, IEEE Trans. Magn. **2**, 305 (1966).

[16] R. C. Alig, R. C. Duncan, Jr., and B. J. Mokross, J. Chem. Phys. **59**, 5837 (1973).

[17] T. S. Piper, J. P. Brown, and D. S. McClure, J. Chem. Phys. **46**, 1353 (1967).

[18] R. Suryanarayanan, J. Ferre, and B. Briat, Phys. Rev. B **9**, 554 (1974).

[19] M. J. Freiser, S. Methfessel, and F. Holtzberg, J. Appl. Phys. **39**, 900, (1968).

[20] R. Suryanarayanan, C. Paparoditis, J. Ferre, and B. Briat, J. Appl. Phys. **43**, 4105 (1972).

[21] L. A. Alekseyeva, N. V. Starostin, and P. P. Feofilov, Opt. Spectrosc. **23**, 140 (1967).

[22] V. Narayanamurti, A. Jayaraman, and E. Bucher, Phys. Rev. B **9**, 9521 (1974).

[23] D. Wohlleben, J. G. Huber, and M. B. Maple, AIP Conf. Proc. **5**, 1478 (1972).

[24] H. R. Ott, K. Andres, and E. Bucher, AIP Conf. Proc. (to be published).

[25] L. L. Hirst, Phys. Kondens. Mater. **11**, 255 (1970).

[26] F. Holtzberg, D. C. Cronemeyer, T. R. McGuire, and S. von Molnar, *Solid Solubility in the Face-Centered-Cubic $Gd_x Se_{1-x}$ System*, Natl. Bur. Stds. Spec. Publ. No. 364 (U. S. GPO, Washington, D.C., 1972), p. 637.

[27] W. Beckenbaugh, J. Evers, G. Güntherodt, E. Kaldis, and P. Wachter, J. Phys. Chem. Solids **36**, 239 (1975); W. Beckenbaugh, G. Güntherodt, R. Hanger, E. Kaldis, J. P. Kopp, and P. Wachter, AIP Conf. Proc. **18**, 540 (1973).

[28] B. Lüthi, P. S. Wang, and E. Bucher (unpublished).

[29] This ratio (for $h\nu \sim 1500$ eV) has been found to correspond well with bulk values inferred by other techniques on other materials. See, e.g., R. A. Pollak *et al.*, Phys. Rev. Lett. **33**, 820 (1974); and M. Campagna *et al.*, *ibid.* **33**, 165 (1974).